# Experiments on Tropical Stratospheric Mean-Wind Variations in a Spectral General Circulation Model

KEVIN HAMILTON

*Geophysical Fluid Dynamics Laboratory/NOAA, Princeton University, Princeton, New Jersey*

LI YUAN

*Atmospheric and Oceanic Sciences Program, Princeton University, Princeton, New Jersey*

(Manuscript received 9 September 1991, in final form 28 February 1992)

ABSTRACT

A 30-level version of the rhomboidal-15 GFDL spectral climate model was constructed with roughly 2-km vertical resolution. In common with other comprehensive general circulation models, this model fails to produce a realistic quasi-biennial oscillation (QBO) in the tropical stratosphere.

A number of simulations were conducted in which the zonal-mean winds and temperatures in the equatorial lower and middle stratosphere were instantaneously perturbed and the model was integrated while the mean state relaxed toward its equilibrium. The time scale for the mean wind relaxation varied from somewhat over one month at 40 km to a few months in the lower stratosphere. This is similar to the time scales of observed QBO wind reversals. The wind relaxations in the model also displayed the downward phase propagation characteristic of QBO wind reversals, and mean wind anomalies of opposite sign to the imposed perturbation appear at higher levels. In the GCM, however, the downward propagation is clear only above about 20 mb.

Detailed investigations were made of the zonal-mean zonal momentum budget in the equatorial stratosphere in these experiments. The mean flow relaxations above 20 mb were mostly driven by the vertical Eliassen–Palm flux convergence. The anomalies in the horizontal Eliassen–Palm fluxes from extratropical planetary waves, however, were found to be the dominant effect forcing the mean flow back to its equilibrium at altitudes below 20 mb. The vertical eddy momentum fluxes near the equator in the model were decomposed using space–time Fourier analysis. While total fluxes associated with easterly and westerly waves are comparable to those used in simple mechanistic models of the QBO, the GCM has its flux spread over a very broad range of wavenumbers and phase speeds.

The effects of vertical resolution were studied directly by repeating part of the control integration with a 69-level version of the model with greatly enhanced vertical resolution in the lower and middle stratosphere. The results showed that there is almost no sensitivity of the simulation in the tropical stratosphere to the increased vertical resolution.

## 1. Introduction

The general circulation in the tropical lower stratosphere has presented particularly difficult challenges to dynamical meteorologists. The observed quasi-biennial oscillation (QBO) of the mean zonal wind has been reproduced in simple mechanistic models (Lindzen and Holton 1968; Holton and Lindzen 1972; Plumb 1977; Plumb and Bell 1982; Dunkerton 1983; Saravanan 1990). These model results show that the mean-flow accelerations in the QBO can be forced by interaction with vertically propagating waves, but also raise questions about the possible role of planetary waves of extratropical origin and the diabatic meridional circulation. Observations are of only limited use in diagnosing the details of the QBO forcing mechanisms [the early work of Lindzen and Tsay (1975) may still be the only quantitative diagnostic study]. The relatively sparse tropical radiosonde network, the rather short vertical scales of the waves thought to be important in the QBO, and the breakdown of geostrophic balance (thus limiting the utility of satellite temperature observations) are all significant complicating factors.

Unfortunately, the study of the tropical lower stratosphere has not been greatly assisted by general circulation models (GCMs). Apparently, no comprehensive GCM has managed to produce anything approaching a realistic QBO. This fact is somewhat puzzling since, in at least some GCMs, the existence of vertically propagating equatorial waves has been documented (Hayashi 1974; Hayashi et al. 1984; etc.).

It is easy to suggest several possible reasons for the inability of GCMs to simulate the QBO. The limited vertical resolution of such models is not adequate to

*Corresponding author address:* Dr. Kevin Hamilton, Princeton University, GFDL/NOAA, P.O. Box 308, Princeton, NJ 08542.

treat vertically propagating waves when their intrinsic frequency (and hence vertical wavelength) becomes small. Unfortunately, there seems to be no definitive indication of how the inadequacy of vertical resolution would actually affect the simulation of wave–mean flow interaction in a model with realistic wave dissipation.

Simulation of a QBO requires that a small, but sustained, mean-flow acceleration be maintained for periods of several months. Sufficiently strong parameterized mean-flow diffusion could suppress the QBO, even if a model had waves strong enough to produce realistic magnitudes for the mean-flow driving (this is apparent in simple models; e.g., Plumb 1977). The strength of the vertically propagating tropical waves generated by GCMs is also important. Models with waves that are significantly weaker than those in the real world will presumably have mean-flow oscillations of very long period (or oscillations that are easily suppressed by mean-flow damping).

Typically the equatorial winds in the lower stratosphere in GCM simulations appear to be "stuck" in a (usually fairly weak) easterly regime (e.g., Manabe and Hunt 1968; Kasahara and Sasamori 1974; Hayashi 1974; Manabe and Mahlman 1976; Boville 1985; Boville and Randel 1986; Hamilton and Mahlman 1988). This fact by itself is consistent with two extreme scenarios: either a strong dynamical constraint holding the winds at a particular value, or a regime of such weak dynamical forcing that no significant mean-flow accelerations can occur. A more hopeful possibility would be a model with a dynamical regime that lies between these very unrealistic extremes.

The present paper reports on a series of numerical experiments designed to investigate the performance of a GCM in the tropical lower stratosphere. A spectral GCM with roughly 2-km vertical resolution up to the stratopause was constructed. It was verified that in a two year control run the equatorial stratospheric zonal-mean winds below 10 mb remain virtually constant (consistent with the behavior seen in earlier GCM studies). The model mean wind and temperature fields were then artificially perturbed and the wave and mean-flow response studied. The analysis showed that the model responded in a somewhat realistic fashion, in terms of the time scale and vertical structure of the resulting mean-flow accelerations. The vertical wave fluxes were also found to adjust to the mean-flow changes in a manner consistent with theoretical expectations. This demonstration that the dynamics in the model tropical stratosphere has some reasonable features encouraged further analysis of both the perturbed and control integrations.

A number of issues were investigated using these model results. The significant tropical vertical momentum transports were shown to be due to waves with a very broad range of horizontal scales and zonal phase velocities. The momentum transport associated with stationary planetary waves propagating from the midlatitudes was also found to be an important component of the zonal-mean momentum balance in the tropical lower and middle stratosphere. The modulation of such stationary planetary waves by the imposed perturbations in the tropical mean flow was studied.

Another experiment was performed to directly investigate the effects of vertical resolution on the equatorial dynamics in the model. In particular, four months of the control integration were repeated with a version of the GCM with considerably enhanced resolution in the stratosphere (about 2/3-km level spacing). Rather surprisingly, the evolution of the tropical stratospheric winds was virtually unaffected by this change in model resolution.

The outline of this paper is as follows. The model and the control integration are briefly described in section 2. The mean-flow evolution in the perturbation experiments is presented in section 3. The detailed analysis of the experiments is described in section 4. Section 5 then describes the high-resolution integrations. The conclusions are summarized in section 6.

## 2. Model and control integration

The model used here was adapted from the spectral GCM developed at GFDL for climate studies. The basic description of the model numerics is given by Gordon and Stern (1982). The model includes topography, a realistic treatment of radiation, and a prognostic equation for water vapor as well as a simple ground hydrology. The radiative transfer code uses climatological ozone values (see Fels et al. 1980) and only diurnally averaged heating rates are computed. Dry and moist convective adjustment are applied at each time step to adjust the temperature profile and determine the precipitation rate. A version of this model with 9 sigma levels has been used at GFDL over the last decade in a number of climate studies, most involving coupled ocean models and/or schemes for predicting cloud cover. For the present study the model was simplified to include prescribed zonal-mean clouds and climatological (but seasonally varying) sea surface temperatures as described in Manabe et al. (1979). The present version of the model also eliminated the subgrid-scale parameterization of gravity wave drag that has been included in many of the more recent climate experiments. While the 9-level version of the climate model has been run with various horizontal resolutions, all calculations in this work were performed with rhomboidal truncation out to zonal wavenumber 15 (the corresponding Gaussian grid for this resolution is 7.5° longitude by roughly 4.5° latitude).

In the present project a 30-level version of the model was constructed. The level structure adopted is shown in Fig. 1 (along with the standard 9-level version used in earlier climate studies and, for comparison, the 40 levels used in the GFDL "SKYHI" troposphere–stratosphere–mesosphere GCM). The top 28 levels are

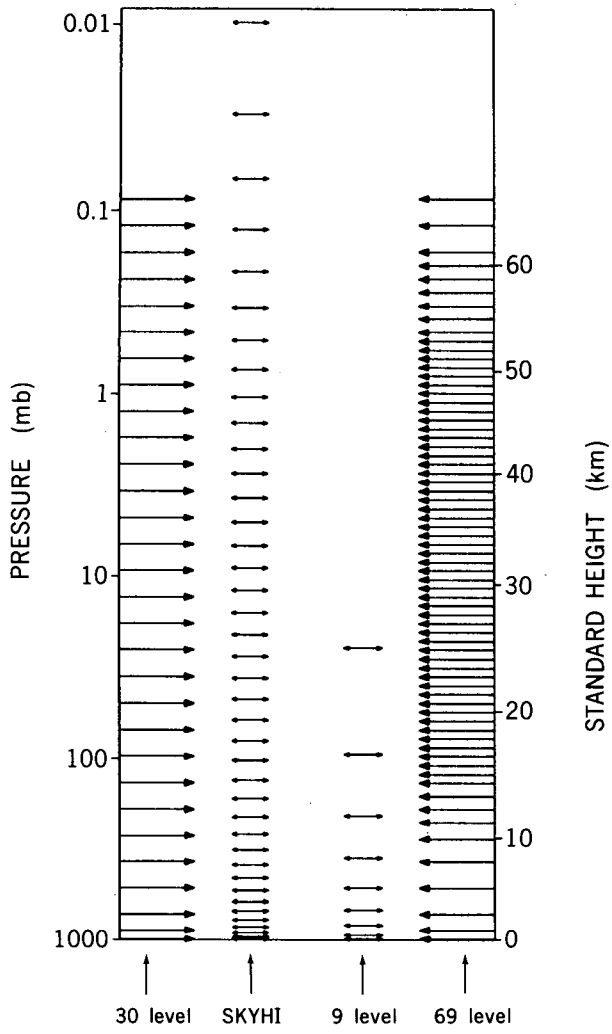


FIG. 1. Level structures of various general circulation models as a function of pressure (assuming a surface pressure of 1000 mb). The column on the left gives the structure for the 30-level model used in this study, while on the right is shown the structure of the 69-level version of this model. For comparison are also shown the level structures for the 9-level spectral model of Manabe et al. (1979) and the 40-level "SKYHI" gridpoint model of Fels et al. (1980).

equally separated in logarithm of sigma (corresponding roughly to a 2-km spacing). The lowest level was chosen to be at nearly the same height as in the 9-level version (since the same exchange coefficients with the ground were adopted). The pure sigma-level coordinate of the original model was retained. While a hybrid scheme that deforms into pressure coordinates at high levels would no doubt be preferable (e.g., Fels et al. 1980; Boville 1985), no obvious problems resulted from the use of pure sigma coordinates in this study. Isobaric maps of the model wind or geopotential fields in the stratosphere (interpolated in a straightforward manner from the model sigma levels) invariably looked quite reasonable. Of course, one limitation of the use of sigma coordinates is the introduction of interpolation errors into isobaric budget calculations (such as the zonal-mean zonal momentum budget; see section 4).

The subgrid-scale dissipation in the model was taken from Manabe et al. (1979). The only vertical mixing (in addition to the convective adjustment of temperature and moisture fields) is in the lowest three levels, where a simple mixing-length formulation is used. The horizontal mixing is parameterized with a $\nabla^4$ diffusion with constant coefficient of $10^{16}$ m$^4$ s$^{-1}$. This means that the model stratosphere can be considered quite inviscid even for QBO time scales. The time for the horizontal diffusion to significantly damp an equatorial jet with 1500-km meridional scale ($\sim$14° latitude) is of the order of 10 years. Thus, it is unlikely that the subgrid-scale dissipation in this model prevents the simulation of a QBO. The subgrid-scale diffusion terms also should not play a significant role in the zonal mean momentum budgets discussed in section 4.

A linear damping of the vorticity and divergence was added in the upper six levels of the model in order to avoid spurious downward reflection of waves as well as to produce a reasonable extratropical jet structure (without this damping the polar night jet becomes unrealistically strong in the top levels). The damping rates in these levels increased from (32 day)$^{-1}$ at level 6 to (2 day)$^{-1}$ at the top level.

The 30-level model was integrated from an isothermal resting state for 30 months beginning 1 January. The evolution of the equatorial zonal-mean zonal wind, $\bar{u}$, is shown in Fig. 2. After January and February of year 1, the tropical lower stratosphere settles into a very steady pattern of weak easterlies, while near 1 mb there is a fairly well developed semiannual oscillation.

Figure 3 shows the monthly mean sea level pressure and the heights of the 500-mb and 10-mb surfaces averaged over January of year 2. The tropospheric fields are quite similar to those simulated in the 9-level model (Manabe et al. 1979) and are in reasonable agreement with observations (Crutcher and Meserve 1970; Taljaard et al. 1969). The 10-mb height field shows a wavenumber one pattern with a well-developed Aleutian high. Northern Hemisphere extratropical stationary wave amplitudes for both wave one and two are comparable to those in observed climatologies. The cross section of the zonal-mean zonal wind fields for December of year 1 are shown later in Fig. 14. The December winds look quite reasonable in both the troposphere and stratosphere, although the separation between the tropospheric and polar night jets is not as pronounced as it is in observations. A similar pattern (although with a slightly stronger polar night jet) is found in Southern Hemisphere winter.

The zonal-mean temperature structure (not shown) was quite realistic, except in the top few levels of the model where temperatures were unrealistically cold (the radiative transfer code was not designed to work at very low pressures). These problems are confined

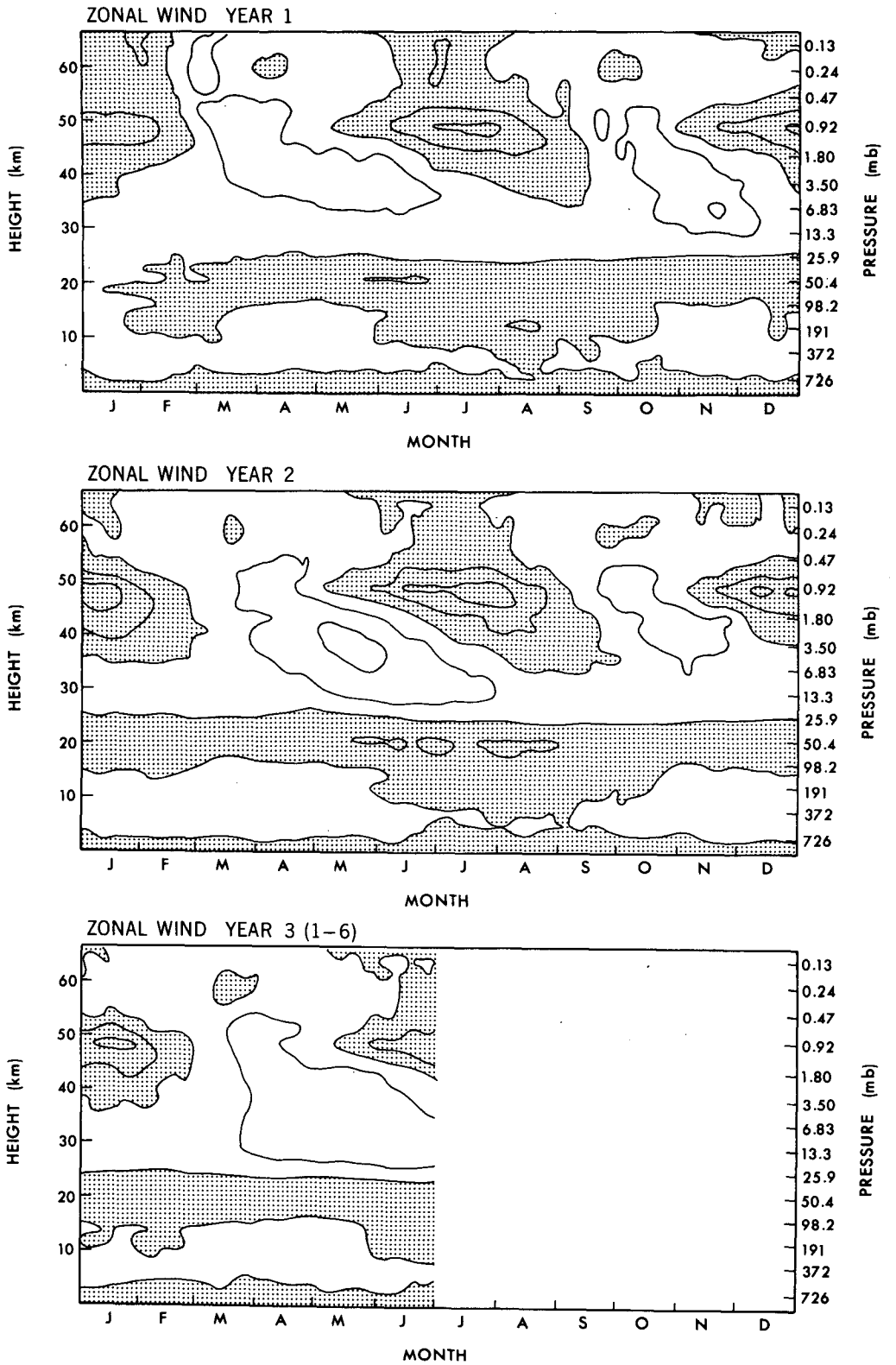


FIG. 2. Time–height section of the equatorial zonal-mean zonal wind in the control run of the 30-level model. These results have been slightly smoothed by taking a running mean over 11 consecutive daily snapshots. The contour interval is 10 m $s^{-1}$ and easterlies are shaded.

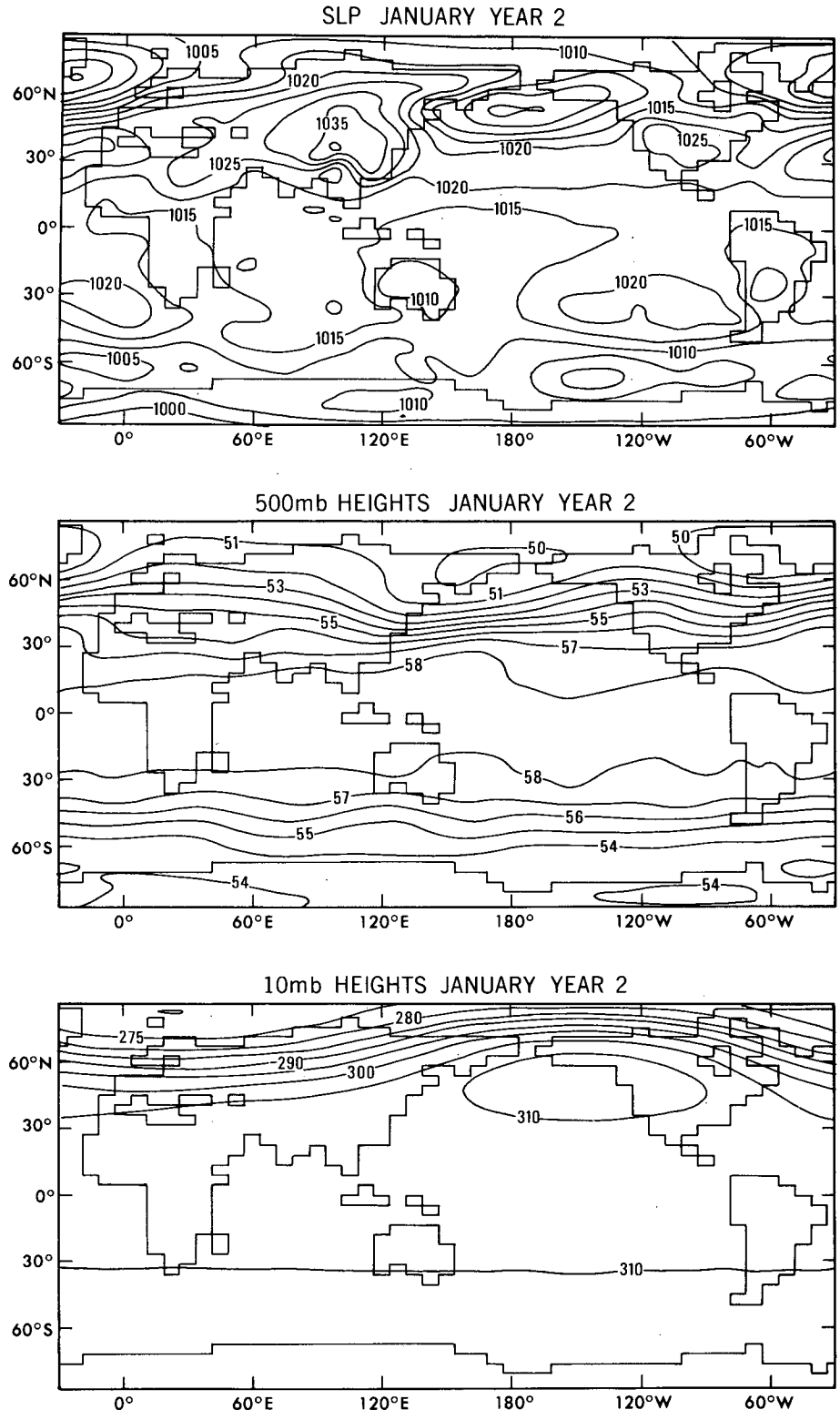


FIG. 3. Monthly mean results from the second January of the control run. The top panel shows the sea level pressure with 5-mb contour interval. The middle and lower panels show the 500-mb and 10-mb heights with contour labels in 100s of m.

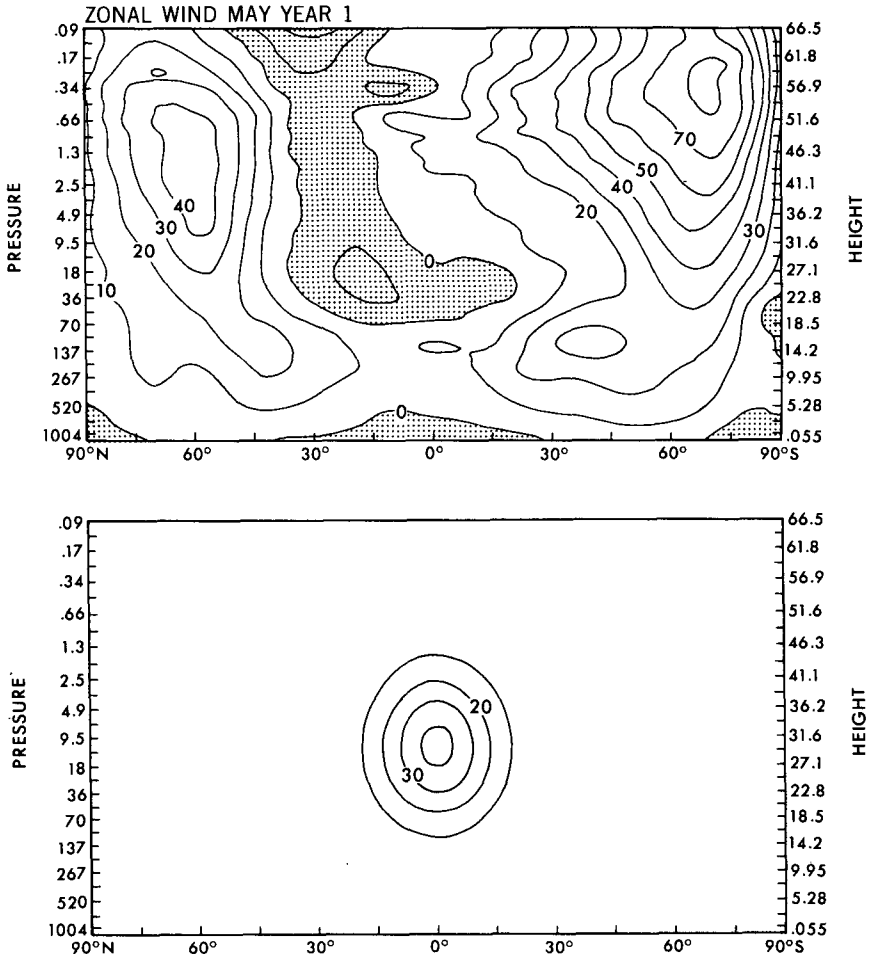


FIG. 4. Top panel: An instantaneous section of the zonal-mean zonal wind on 1 May of the year 1 of the control run. The contour interval is 10 m $s^{-1}$ and easterlies are shaded. Lower panel: The mean wind anomaly introduced in the perturbation experiments. Again the contour interval is 10 m $s^{-1}$.

to the "sponge" region at the top where there is no direct interest in the simulation.

## 3. Perturbation experiments

The top panel of Fig. 4 shows the zonal-mean zonal wind on 1 May of the first year of integration. The full three-dimensional model fields at this instant were altered by the addition of a strong zonal-mean jet centered at the equator and near 10 mb (see the bottom panel of Fig. 4). The zonal-mean temperature field was also altered by adding a perturbation that was in thermal wind balance with the wind and had zero horizontal mean at each level. This altered field was then used as the initial condition for a 120-day integration. This experiment was performed with a westerly wind perturbation and then repeated for an easterly perturbation. Inspection of the zonal-mean fields and horizontal maps at daily intervals through the first days of the integrations revealed no obvious anomalies that might have been caused by residual imbalance in the initial conditions.

Figure 5 shows the time–height section of the equatorial zonal wind in the perturbed experiments minus that in the control integration. The top is for the easterly perturbation experiment and the bottom is for the westerly perturbation run. (Since the equatorial mean winds over the lower and middle stratosphere in the control run are fairly weak, plots of the actual wind evolution in the perturbation experiments look rather similar to the anomaly plots in Fig. 5.)

At first glance, the results in Fig. 5 appear to be fairly encouraging. The wind anomaly introduced in the initial conditions is largely destroyed by the end of the 120-day period. Above about 20 mb the results are particularly realistic, with an apparent downward propagation of the shear zone and the formation of an anomaly of the opposite sign at higher levels. The re-

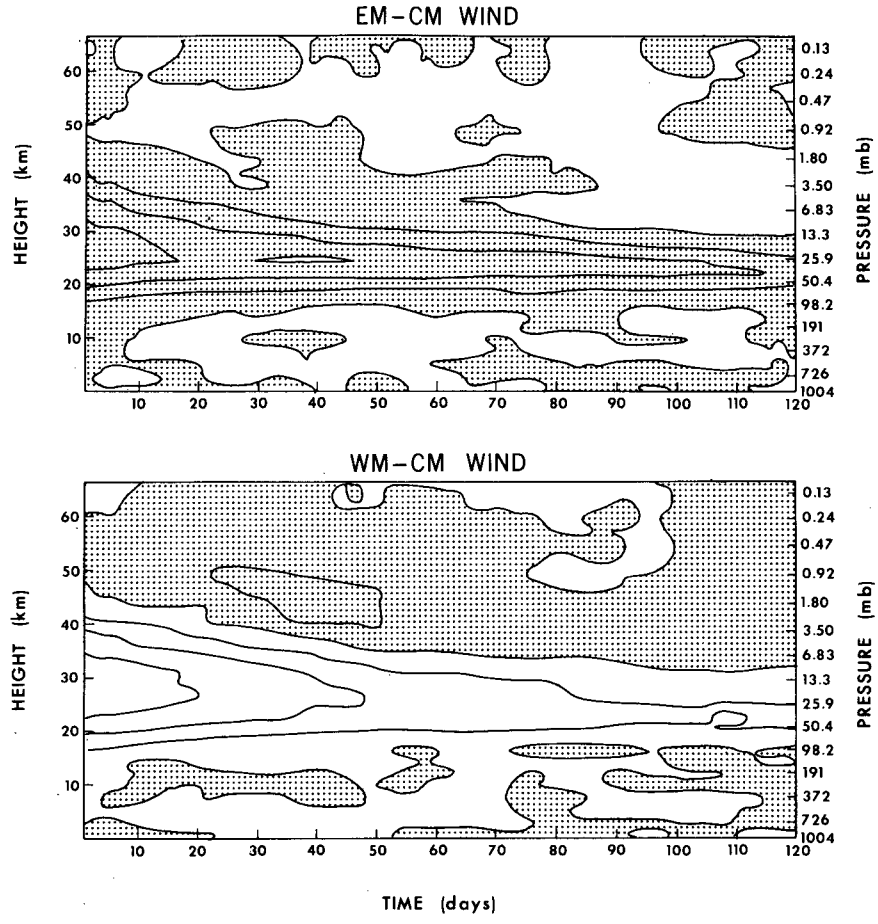


FIG. 5. Top panel: The equatorial zonal-mean zonal wind in the easterly perturbed experiment begun on 1 May minus that in the control integration. The contour interval is 10 m $s^{-1}$ and negative values (i.e., anomalously easterly winds) are shaded. An 11-day running mean has been applied. Bottom panel: The same quantity but for the westerly perturbation experiment.

sults off the equator are fairly similar in general form, that is, there is little evidence for meridional phase propagation of the accelerations.

The results below about 20–30 mb, and most particularly near 40 mb, are less impressive. The accelerations are quite weak and little evidence of downward propagation is evident. This problem is particularly severe in the easterly perturbation experiment, where a wind anomaly of almost 20 m $s^{-1}$ persists at 40 mb even at the end of the integration.

Overall, the westerly anomalies relax more quickly than the easterly anomalies. This is unlike the observed QBO in which the westerly accelerations tend to be more abrupt than the easterly accelerations. [Note that Dunkerton (1991) has recently considered the issue of asymmetry of QBO shear regimes using a nonlinear axisymmetric model.]

The easterly and westerly perturbation experiments were repeated for initial conditions on 1 December of the first year of control integration. The results for the equatorial wind anomalies are shown in Fig. 6. The overall picture is the same as in the May experiment, although the wind relaxations occur a little faster in the December experiments. The most impressive results are for the westerly perturbation case, where a descending easterly anomaly greater than 10 m $s^{-1}$ forms above the westerly jet and persists until the end of the 120-day experiment.

The perturbation experiments were repeated starting from 1 December of the second year of control integration (on the assumption that there could be significant interannual variability in the Northern Hemisphere winter stratospheric circulation). The results for the equatorial wind anomalies (not shown) were very similar to those in Fig. 6.

The perturbation experiments are perhaps the simplest that can be devised in terms of the geometry of the imposed wind anomaly. Of course, the introduction of a single jet produces an initial condition that really does not resemble any phase of the observed QBO. The perturbation experiment for May was repeated with an imposed anomaly consisting of a westerly jet

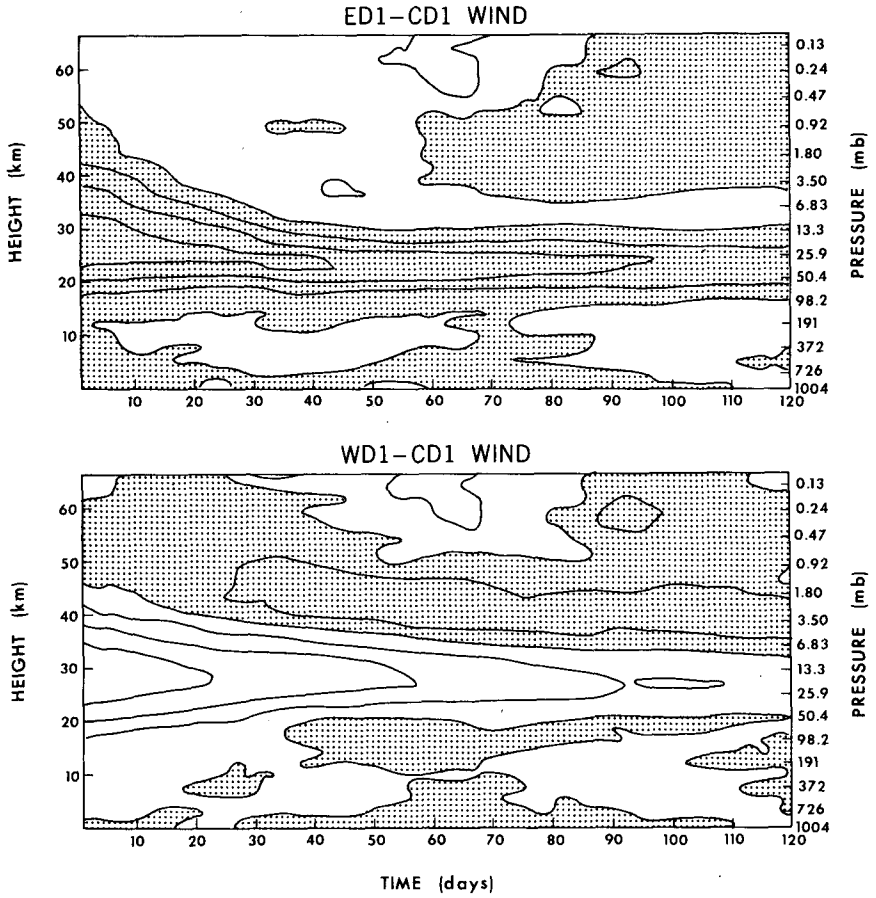


FIG. 6. As in Fig. 5 but for perturbation experiments started on 1 December of year 1.

overlying an easterly jet and then repeated again for the opposite polarity (of course, since the mean-flow perturbations are introduced suddenly without adjusting the waves, even this is not a perfect representation of an instant in a QBO cycle). The results (not shown) were similar to those of the simpler perturbation experiments. The wind anomalies had largely disappeared by the end of the 120-day integration period. Just as in the single jet perturbation experiments, the relaxation was faster at higher levels. There was little indication of downward propagation of mean wind regimes in the lower stratosphere.

## 4. Detailed analysis of the model response to the mean wind perturbation

### *a. Momentum budget*

During the control and perturbation integrations, snapshots of the model fields (including the pressure vertical velocity, $\omega$, computed from the model divergence field) were saved once per day. These were interpolated (linearly in log-pressure) from the 30 sigma levels to the corresponding isobaric levels. The results allowed a fairly complete diagnosis of the eddy fluxes and their effects on the mean flow. Results for the height–latitude structure of eddy flux divergences tend to be somewhat noisy, however. This is at least partly due to time sampling problems (similar to those found in the diagnosis of the middle atmosphere results in Hamilton and Mahlman 1988). For both the control run and the perturbation experiments the months of May and December (i.e., when the perturbations to the mean flow and to the wave fluxes are largest) were rerun with sampling roughly ten times per day. The computed flux divergences were then much smoother, particularly when some averaging in latitude was performed. The analysis discussed in this section will deal with the results in May and December. Similar analysis for the entire 120 days of the perturbation experiments (using the once-a-day sampling) leads to essentially the same conclusions.

Figures 7–9 show the components of the transformed Eulerian (TE) zonal momentum budget averaged over the region 13.5°S–13.5°N for May in the control integration and in each of the perturbed experiments. Figure 7 is for the control integration; Fig. 8 (Fig. 9) is for the difference between the easterly (westerly) perturbed experiment and the control run.

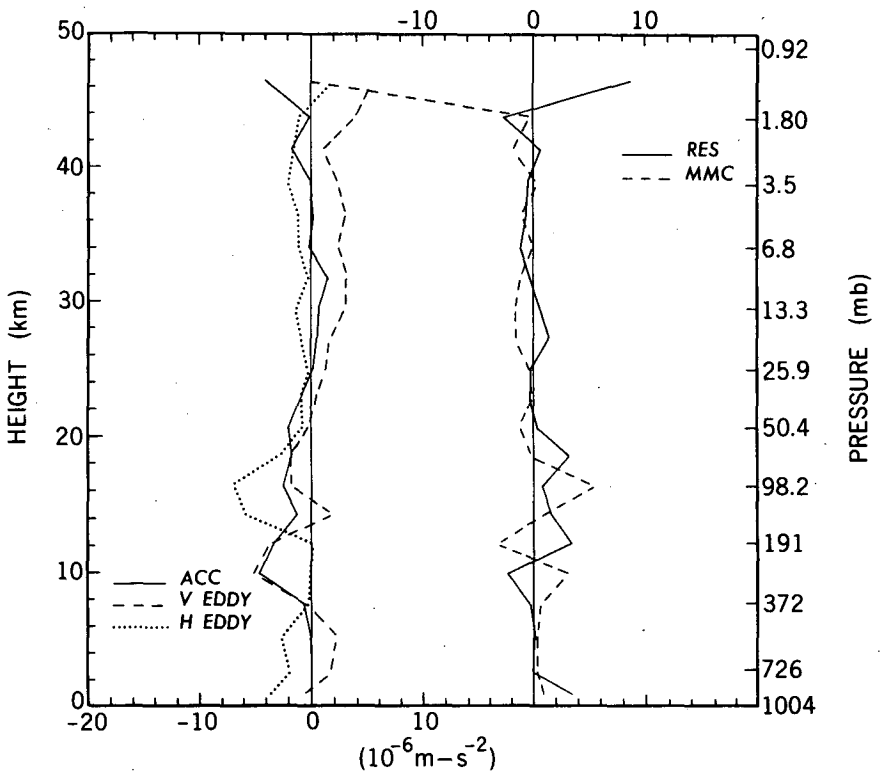


FIG. 7. Components of the transformed Eulerian zonal momentum budget in the control integration averaged over May of year 1. The various terms shown are the mean-flow acceleration (ACC), the contribution from the vertical EP flux convergence (V EDDY), the contribution from the horizontal EP flux convergence (H EDDY), the contribution from advection by the residual mean meridional circulation (MMC), and the residual needed to balance the budget (RES). Note that the scale for the MMC and RES terms is given at the top of the graph. Results are shown up to the third level below the sponge layer.

The various terms are expressed in acceleration units and are defined as follows:

ACC: acceleration of the mean zonal wind
V EDDY: contribution from vertical Eliassen–Palm (EP) flux divergence
H EDDY: contribution from horizontal EP flux divergence
MMC: contribution from advection by the residual mean meridional circulation
RES: a residual equal to acceleration, ACC, minus the sum of V EDDY, H EDDY, and MMC contributions.

Under ideal circumstances the residual, RES, plus the contribution from subgrid-scale mixing (small except near the ground) should be zero. The nonzero residuals are presumably due to a combination of (i) the interpolation from sigma coordinates, (ii) the imperfect sampling (note that ACC is computed by differencing the wind at the beginning and end of the month, while the other terms are means over the ten snapshots per day), and (iii) the use of finite differences applied to the zonal momentum equation in the diagnostic analysis versus the spectral solution of the vorticity and divergence equations in the model. It is apparent from the figures that these errors can be quite significant, particularly in the troposphere and in the top few levels below the sponge layer. Fortunately, in the region of principal interest (20–40 km) the RES term in the perturbation experiments is typically only 20% of the actual accelerations.

The largest mean-flow accelerations in the perturbed experiments are between 30 and 40 km (10–3 mb), where they approach 1 m $s^{-1}$ $day^{-1}$ (consistent with the mean-flow relaxation seen during the first month in Fig. 6). In this region the anomaly in the vertical EP flux divergence can account for most of the mean-flow changes. The meridional circulation term is rather small and has a noisy vertical structure, but the horizontal EP flux divergence makes a significant contribution (typically 50% of the vertical flux convergence at most levels). The contribution from the vertical EP flux divergence drops off rapidly below 30 km and in the lower stratosphere most of the force that acts to restore the mean flow comes from the horizontal EP flux divergence.

Figure 10 shows the same analysis applied to the westerly perturbed experiment in December of year 1.

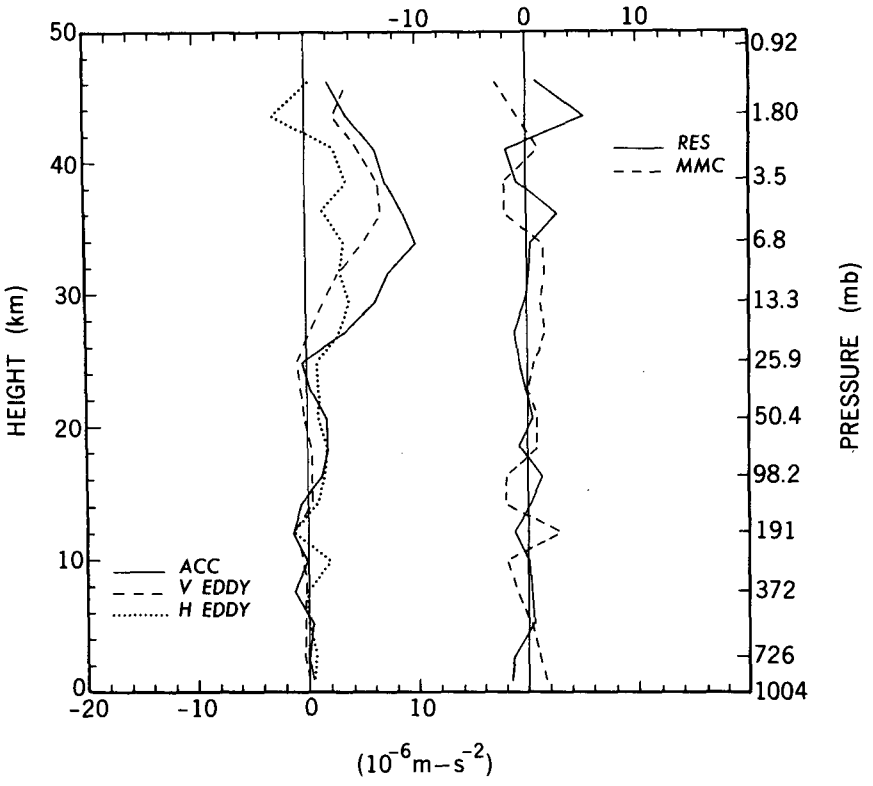


FIG. 8. As in Fig. 7 but each term is now the difference between that in the easterly perturbed experiment and that in the control run.

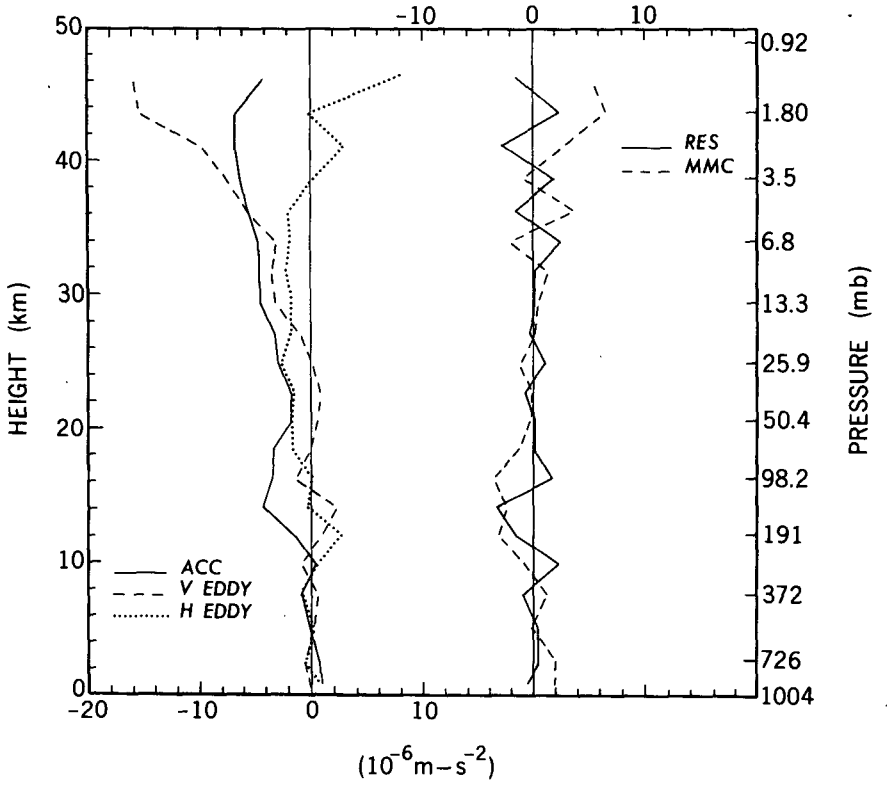


FIG. 9. As in Fig. 7 but each term is now the difference between that in the westerly perturbed experiment and that in the control run.

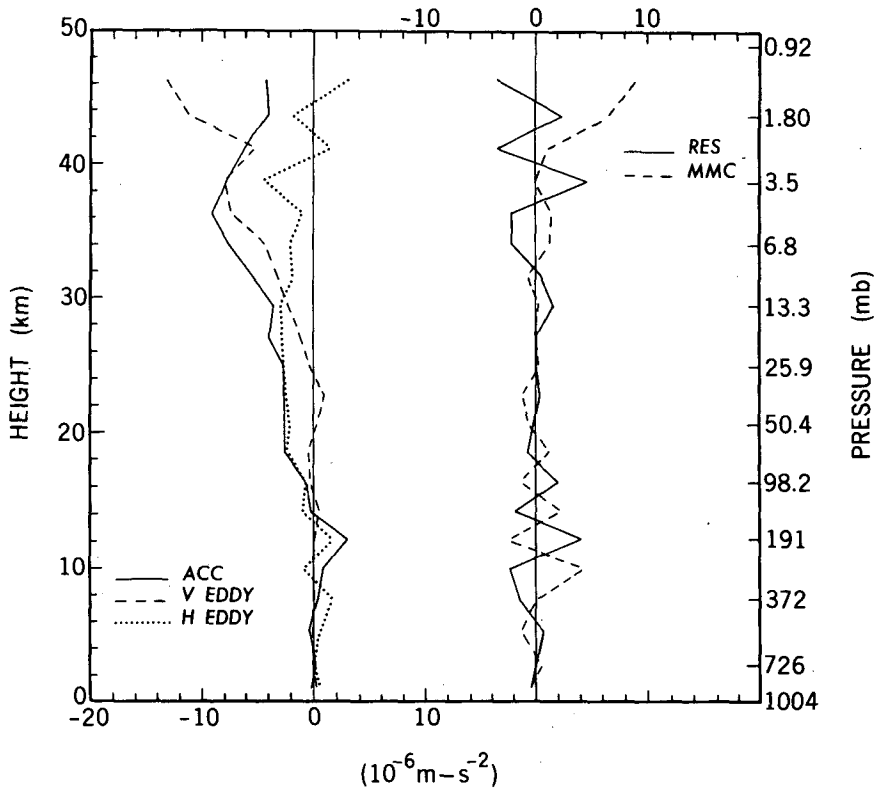


FIG. 10. As in Fig. 9 but for December of year 1 in the experiment with the westerly perturbation.

These results and those for the corresponding easterly perturbed experiment (not shown) are similar in most respects to those seen in May. In the perturbation experiments the relaxation of the winds is strongest above 30 km where it is principally forced by the vertical EP flux divergence. Below about 30 km the horizontal eddy fluxes play the dominant role.

Figure 11 shows the height–latitude structure of the EP flux in the December perturbation experiments minus that in the control integration. The fluxes have been computed using the log-pressure formalism and sign convention of Dunkerton et al. (1981). The vectors plotted have been scaled by the mean density and vertical components are scaled arbitrarily relative to horizontal components. Throughout the 20–40-km range in the westerly perturbed experiment there is an increase in the EP flux reaching into the equatorial region from the Northern Hemisphere extratropics. There is a corresponding reduction of this flux in the easterly perturbed experiment as indicated by the flux of arrows northward in the top panel of Fig. 11. In the equatorial region the perturbation to the vertical component of the flux is particularly evident, with the downward orientation of the arrows in the easterly perturbed experiment indicating an enhanced upward flux of westerly waves (and the opposite for the westerly perturbed experiment shown in the bottom panel). The results for the May perturbed experiments (not shown) are similar, although in that case the perturbations in the equatorward component of the EP flux are much more symmetric between the two hemispheres.

### *b. The vertical wave fluxes*

The finding that the tropical mean wind perturbations at sufficiently high altitudes are reduced by vertical eddy momentum fluxes is consistent with expectations based on the theory of vertically propagating internal waves (e.g., Lindzen 1971; Holton and Lindzen 1972; Plumb 1977). For example, when anomalous mean westerlies are present in the stratosphere, waves with westerly phase speed have smaller vertical group velocity than in the control run. Thus, westerly waves should be dissipated more strongly and a net anomalous easterly wave flux should be present at higher levels. As shown by Lindzen and Holton (1968) and Holton and Lindzen (1972), this kind of "wave shadow" effect leads to induced mean-flow accelerations that can have apparent downward phase propagation with height.

The vertical flux convergence term in the TE momentum balance (V EDDY terms in Figs. 7–10 above) was found to be generally within about 20% of the corresponding vertical eddy momentum flux conver-

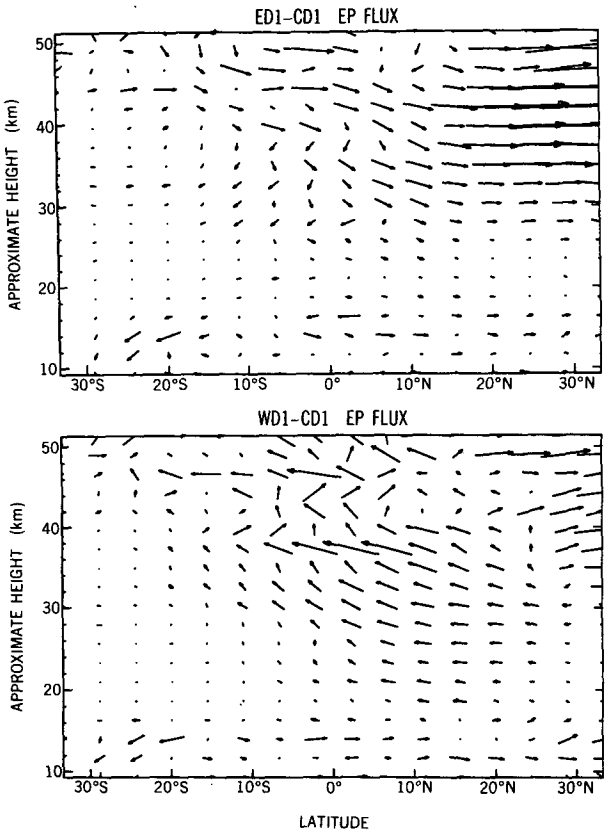


FIG. 11. Change in the EP flux between the December easterly perturbed experiment and control (top), and between the December westerly perturbed experiment and control (bottom). The vectors represent EP flux defined in log-pressure coordinates by Dunkerton et al. (1981) divided by the mean density. Results are shown for each model level between 0.66 mb and 267 mb. The scale is such that a horizontal vector the length of a ten-degree interval represents 4 $m^2 s^{-2}$ times the earth's radius. The same-length vertical vector would represent 0.025 $m^2 s^{-2}$ times the earth's radius.

gence per unit mass. Thus, the more detailed analysis in this section will focus on the Eulerian vertical eddy momentum fluxes. Figure 12 shows the equatorial value of the vertical eddy momentum flux, $\overline{u'\omega'}$, at 13.3 mb partitioned among the 15 zonal wavenumbers for the control experiment in May and in the corresponding westerly perturbed and easterly perturbed experiments. In the control run the net wave fluxes are dominated by the large-scale waves (say, wavenumbers 1–5). By contrast, however, the alteration in the fluxes in the perturbed experiments is large at all horizontal scales. This is true at other levels, as can be seen in Fig. 13, which shows the difference in $\overline{u'\omega'}$, between the westerly perturbed and control experiments divided among zonal wavenumbers for each of the stratospheric levels (results for the easterly perturbation are similar but with the opposite sign). Since the vertical group velocity for the largest-scale waves is of the order of a kilometer per day, the wave field in the middle and upper stratosphere may take some time to adjust to

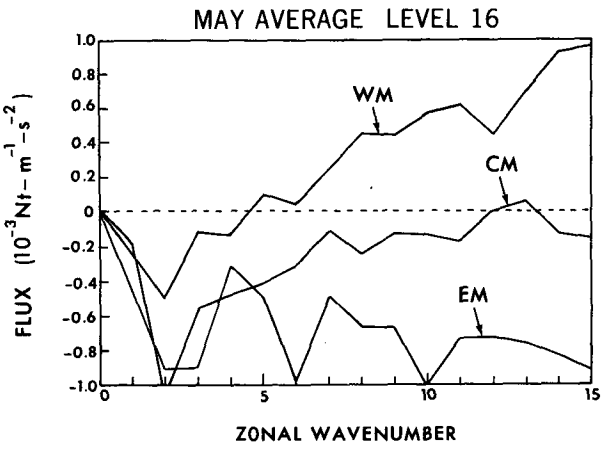


FIG. 12. Equatorial flux $\overline{u'\omega'}$ at the 13.3-mb level (i.e., the pressure value corresponding to level 16 of the model) divided among zonal wavenumbers. The curve CM is an average for the control integration in May of year 1, while WM and EM are for the corresponding westerly and easterly perturbation experiments.

the sudden mean-flow perturbation introduced on 1 December. To address this issue the spectral analysis of the momentum fluxes shown in Figs. 12 and 13 was repeated using just the data in 16–30 December. The results (not shown) are very similar.

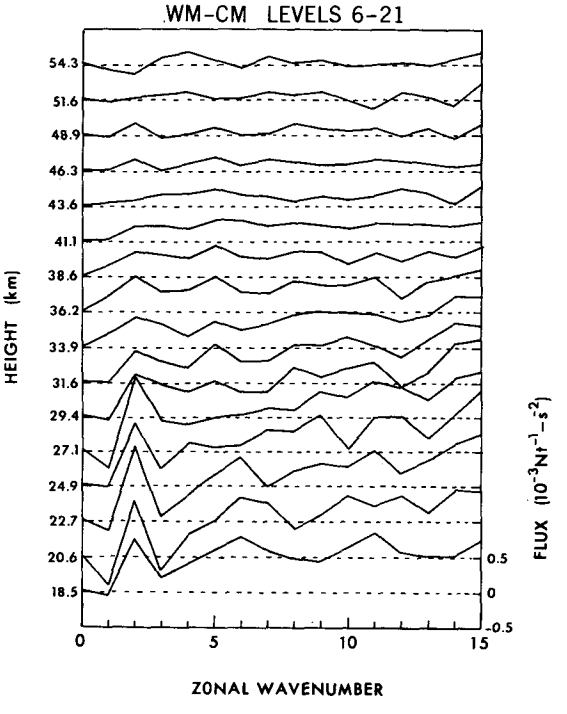


FIG. 13. Difference in the equatorial flux $\overline{u'\omega'}$ between the westerly perturbed and control experiments in May divided among zonal wavenumbers. Each curve represents results at one pressure level corresponding to the one of the model levels 6 through 21 (0.47 mb to 70.4 mb).

TABLE 1. Equatorial vertical eddy momentum fluxes, $-\overline{u'\omega'}$, at the isobaric levels corresponding to model levels 21 and 16 partitioned into zonal wavenumber and zonal phase-speed intervals. Phase-speed intervals are in m $s^{-1}$ and easterlies are negative. Fluxes are in $10^{-4}$ N $m^{-1}$ $s^{-1}$ and positive values correspond to the upward transport of westerly momentum. Results for May of the control run.

| | Phase speeds | | | | | | | | |
|---|---|---|---|---|---|---|---|---|---|
| Wavenumbers | <−75 | −75 −50 | −50 −25 | −25 0 | 0 25 | 25 50 | 50 75 | >75 | Total |
| | | | | 70.4 mb (level 21) | | | | | |
| 1–5 | −4.6 | −2.2 | 0.3 | −0.9 | 8.4 | 32.4 | 11.9 | 7.5 | 52.8 |
| 6–10 | −0.8 | −3.0 | −6.4 | −1.1 | 10.2 | 14.0 | 5.7 | 0.8 | 19.5 |
| 11–15 | −0.2 | −1.1 | −4.4 | −4.7 | 17.8 | 7.2 | 1.9 | 0.1 | 16.7 |
| | | | | 13.3 mb (level 16) | | | | | |
| 1–5 | −3.3 | −1.2 | 0.0 | 0.8 | 2.9 | 9.8 | 13.5 | 4.4 | 26.9 |
| 6–10 | −0.9 | −3.1 | −6.0 | −0.8 | 3.2 | 11.5 | 4.4 | 1.1 | 9.3 |
| 11–15 | −0.1 | −0.8 | −4.8 | −5.6 | 5.9 | 7.9 | 1.5 | 0.2 | 4.1 |

For further analysis the wind fields along the equator were decomposed into a space–time spectrum of traveling waves using the technique of Hayashi (1971). The covariance $\overline{u'\omega'}$, was then partitioned into various zonal wavenumber and zonal phase-speed intervals. The results are shown in Table 1 for the control integration in May (note that the quantities in this table are defined as $-\overline{u'\omega'}$, and so can be regarded as the net upward eddy flux of westerly momentum). The results are shown for two isobaric surfaces, one near level 21 (70 mb) and one near level 16 (13.3 mb).

The control results in Table 1 are consistent with the view that the eddy fields are largely dominated by upward-propagating internal waves. In particular, the waves with westerly (easterly) phase speed are generally associated with a positive (negative) value of the momentum transport. At 70.4 mb the total flux associated with westerly waves is 0.0117 N $m^{-1}$ $s^{-2}$ and the total flux associated with easterly waves is −0.0028 N $m^{-1}$ $s^{-2}$. These numbers are comparable to the values of about ±0.005 N $m^{-1}$ $s^{-2}$ imposed for both the easterly and westerly wave EP fluxes at the 17-km level in the simple QBO model of Holton and Lindzen (1972). The dominance of westerly waves over easterly waves leads to a net westerly forcing from the vertical eddy momentum flux convergence at all heights above about 20 km (see Fig. 7). This westerly forcing is opposed by an easterly mean flow driving from the horizontal eddy flux convergence (Fig. 7).

While the total vertical wave fluxes seen in the control GCM integration are comparable to those imposed in the Holton–Lindzen model, the spectral distribution is very different. The fluxes in the GCM simulation are spread among a wide range of wavenumbers and phase speeds, while those in the Holton–Lindzen model are concentrated at large horizontal scales and modest (30 m $s^{-1}$) phase velocities. The detailed results in Table 1 even show that the dominance of the low wavenumbers in the *net* flux at level 16 (curve CM in Fig. 13) is largely due to a greater cancellation of the fluxes due to easterly and westerly waves at high wavenumbers.

Table 2 shows the power in the equatorial 70.4-mb meridional and zonal wind partitioned among the same

TABLE 2. The variance of the zonal wind (top) and meridional wind (bottom) partitioned among various zonal wavenumbers and zonal phase-speed intervals. Variances are in $m^2$ $s^{-2}$. Results for the isobaric level corresponding to model level 21 (70.4 mb). Phase-speed intervals are in m $s^{-1}$ and easterlies are negative. Results for May in the control run.

| | Phase speeds | | | | | | | | |
|---|---|---|---|---|---|---|---|---|---|
| Wavenumbers | <−75 | −75 −50 | −50 −25 | −25 0 | 0 25 | 25 50 | 50 75 | >75 | Total |
| | | | | Zonal wind | | | | | |
| 1–5 | 0.8 | 0.6 | 5.3 | 12.9 | 4.6 | 6.9 | 1.8 | 1.0 | 33.9 |
| 6–10 | 0.1 | 0.2 | 0.9 | 5.5 | 3.1 | 1.3 | 0.3 | 0.1 | 11.4 |
| 11–15 | 0.0 | 0.1 | 0.5 | 3.5 | 2.3 | 0.5 | 0.1 | 0.0 | 7.0 |
| | | | | Meridional wind | | | | | |
| 1–5 | 2.5 | 1.2 | 2.4 | 2.6 | 0.4 | 0.6 | 0.7 | 1.9 | 12.3 |
| 6–10 | 0.1 | 0.2 | 1.4 | 8.7 | 1.2 | 0.9 | 0.3 | 0.2 | 12.9 |
| 11–15 | 0.0 | 0.0 | 0.3 | 5.5 | 1.2 | 0.4 | 0.1 | 0.0 | 7.6 |

wavenumber and phase-speed intervals. There is a notable dominance of zonal wind variance over meridional wind variance in most of the intervals, even in those including the classical Yanai–Maruyama (1966) Rossby–gravity wave (i.e., the 1–5 wavenumber range with phase-speed magnitudes $< 50$ m s$^{-1}$). The vertical eddy momentum flux convergence being nearly equal to the vertical EP flux convergence is also consistent with having only a weak easterly Rossby–gravity wave component of the spectrum (e.g., Lindzen 1971).

That so much of the vertical wave momentum flux in the GCM is associated with waves with either large zonal phase speeds or large zonal wavenumbers is relevant to the mean-flow structure of the tropics in the model. For equatorial waves or gravity waves the vertical group velocity generally increases with both the zonal wavenumber and the intrinsic phase speed (for gravity waves or Kelvin waves the group velocity is proportional to the zonal wavenumber and to the square of the intrinsic phase speed). Since the scale height for damping of wave flux should be inversely proportional to the vertical group velocity, it may be that the relatively high group velocity waves in the GCM cannot interact strongly with the mean flow in the stratosphere until they reach heights at which the radiative damping is sufficiently strong. This may explain why the vertical EP flux does not play a significant role in reducing the wind perturbations below about 20 mb (see Figs. 8 and 9). It is reasonable to speculate that the fact that much of the vertical wave momentum flux is associated with high vertical group velocities may be a significant factor in the absence of a QBO in the GCM.

The spectral distribution of low-latitude waves in the GCM is clearly different from that in the simple models of Holton and Lindzen (1972) or Plumb (1977) and Plumb and Bell (1982). Even the mechanistic model of Saravanan (1990), while including a wide range of wave phase speeds, considers only very large zonal scales. It is plausible that the reason the simple models produce a QBO, while the GCM does not, may lie in this difference in wave spectra. The question of how realistic the GCM may be in this regard is not easily answered. There are observational studies indicating the presence of significant wave activity with phase speeds considerably greater than 30 m s$^{-1}$ (e.g., Hirota 1978; Salby et al. 1984).

Table 3 shows how the spectrum of wave momentum flux is modified in the mean wind perturbation experiments. Results are presented for the 13.3-mb level in the May experiments. The changes in the total flux reaching this level is strongest in the 11–15 wavenumber range because the cancellation between easterly and westerly waves is now much less pronounced.

The results expressed in Figs. 12 and 13 and Tables 1 and 3 are similar when the analysis is repeated for the December control and perturbed runs.

The spectrum of vertically propagating waves entering the tropical stratosphere would presumably be dependent on the parameterization of convective heating in the model. The use of an abrupt convective adjustment of each individual column in the present model might intuitively be expected to produce a spectrum rich in high-frequency components. There may be other parameterizations that favor lower-frequency and larger-scale waves. The present analysis suggest that such a parameterization could lead to a more realistic simulation of the tropical stratosphere.

### c. *The quasi-stationary waves*

The tropical zonal-mean momentum budgets revealed that the horizontal eddy momentum fluxes play an important role in dynamics of the mean flow in both the control integration and the perturbed experiments. The horizontal eddy momentum flux convergence computed using the monthly mean fields was typically found to be over 50% of the total, strongly suggesting that the H EDDY term in Figs. 7–10 is to be ascribed largely to quasi-stationary waves. By contrast, less than 10% of the vertical eddy momentum flux convergence is accounted for by the monthly mean eddy field.

TABLE 3. As in Table 1, but for the differences in the momentum flux between the easterly perturbed experiment and the control run (ep-control) and the westerly perturbed experiment and the control run (wp-control). Results for 13.3 mb in May. Units are $10^{-4}$ N m$^{-1}$ s$^{-1}$.

| | Phase speeds | | | | | | | | |
|---|---|---|---|---|---|---|---|---|---|
| Wavenumbers | <−75 | −75 −50 | −50 −25 | −25 0 | 0 25 | 25 50 | 50 75 | >75 | Total |
| | | | | wp-control | | | | | |
| 1–5 | −2.3 | 0.2 | −1.6 | −1.5 | −2.5 | −7.4 | −5.3 | 1.4 | −19.0 |
| 6–10 | 0.1 | −0.3 | −4.0 | −5.9 | −3.7 | −10.7 | −1.7 | −0.3 | −26.6 |
| 11–15 | 0.0 | −0.6 | −2.5 | −15.6 | −12.8 | −7.8 | −0.8 | −0.3 | −40.2 |
| | | | | ep-control | | | | | |
| 1–5 | 0.5 | 1.4 | −1.1 | −0.3 | 4.5 | 1.2 | −3.0 | 0.0 | 3.4 |
| 6–10 | 0.2 | 1.1 | 5.1 | 2.6 | 12.1 | 5.2 | 0.6 | 0.1 | 27.0 |
| 11–15 | 0.0 | −0.3 | 2.7 | 9.1 | 18.5 | 3.6 | 0.8 | −0.2 | 34.2 |

There has been considerable speculation that quasi-stationary planetary waves forced in midlatitudes may be important in the tropical stratosphere (e.g., Dickinson 1969; Andrews and McIntyre 1976; Dunkerton 1983). Topographic forcing in the extratropical troposphere should lead to quasi-stationary waves with easterly phase speeds relative to the mean flow. Such waves will propagate vertically and meridionally in the stratosphere (during the seasons when the mean flow is westerly). Some fraction of the wave activity will refract into the tropical stratosphere. The convergence of the easterly Eliassen–Palm flux associated with these waves will lead to an easterly mean-flow driving in the tropics at the latitudes where the wave dissipates. While the quantitative theory for the mean-flow effects of vertically propagating equatorial or gravity waves is well developed, there is less detailed understanding of how meridionally propagating stationary waves should interact with the mean flow. Simple linear models of stationary waves in realistic mean flows on the sphere are very sensitive to the treatment of dissipation near the critical surface (e.g., Ma 1990). The present perturbation experiments provide a chance to look at the behavior of the stationary wave fields in a rather complete model. Attention will be restricted to the December results, where the source of stratospheric quasi-stationary waves should be essentially restricted to the Northern Hemisphere.

Figure 14 shows the zonal-mean zonal wind averaged over December of year 1 for the control integration and for the perturbed experiments. The introduction of the perturbation clearly leads to a very different mean flow encountered by a wave propagating from the Northern Hemisphere extratropics. Figure 15 shows the December mean zonal wind field at 9.5 mb for the control and perturbation experiments. In all three cases there is a predominantly wavenumber one stationary wave present with clear southwest–northeast phase tilt (corresponding to an easterly momentum transport into the tropics). The penetration of this wave into low latitudes is clearly affected by the mean wind perturbation. In the easterly perturbed experiment the stationary wave has been virtually excluded from the region equatorward of 15°N. In the control run even at the equator there is still a noticeable stationary wave in the zonal wind field. The tropical penetration is even more pronounced in the westerly perturbed experiment, with mean wind contrasts of about 20 m $s^{-1}$ appearing along the equator. Even in this case the wave decays quickly before reaching the zero mean wind line at about 15°S. The general picture seen in Fig. 15 is found at other levels in the lower stratosphere.

Observations suggest that the zonal-mean wind in the QBO may affect quasi-stationary waves not only in the tropics, but also at higher latitudes. In particular, there is evidence that when the prevailing winds in the tropical lower stratosphere are easterly the extratropical winter vortex is more disturbed than when the tropical winds are westerly (Holton and Tan 1980, 1982; Dunkerton and Baldwin 1991). In the present work the extratropical amplitudes of zonal waves one and two were examined in both the December and January means of the control and perturbed runs. This was done for both the perturbation runs begun on 1 December of year 1 and those begun on 1 December of year 2. No clear picture of the effect of mean wind perturbations emerged. The difference between the two control years was typically as great as between the corresponding perturbed and unperturbed integrations. It appears that it would take a much longer set of multiyear integrations to clearly determine the influence of the tropical mean flow on the extratropical stratospheric circulation.

## 5. Increased vertical resolution

The roughly 2-km vertical resolution employed in the present model is clearly inadequate to represent the details of internal wave critical levels. It remains an open question as to how seriously this deficiency will actually affect the simulation of the wave–mean flow interaction in the tropical stratosphere. To investigate this issue directly, another version of the model was constructed with the 69-level structure shown in Fig. 1. This model was designed to have the same tropospheric-level structure as the 30-level model, but to have three times the resolution in the stratosphere. This somewhat peculiar structure is clearly far from the optimum for overall simulation, but it does allow for the direct comparison with the 30-level model discussed later in this section.

The 69-level model was initialized using fields interpolated from the 30-level results on 1 May of year 1. The 69-level model was then integrated through August. Figure 16 shows the zonal-mean zonal wind averaged over the last ten days of June and the last ten days of August for both models. The tropical mean winds in the two simulations are remarkably similar, even after four months. This suggests that the net mean flow driving from tropical waves in the control run (where the mean winds are quite weak) is not significantly distorted by a 2-km vertical resolution.

This conclusion comes with a number of caveats, however. The fact that the 69-level model retained a coarse tropospheric resolution may have limited the generation of waves with small vertical wavelengths. The integrations shown in Fig. 16 had rather weak mean winds throughout most of the tropical stratosphere. It may be that under these conditions most of the vertical wave fluxes are associated with waves far from their critical phase speeds. Also, it is conceivable that models with different formulations for wave dissipation or models with finer horizontal resolution might behave differently. Finally, one could argue that even 2/3 km level spacing is woefully inadequate to resolve parts of the wave spectrum, and that significant

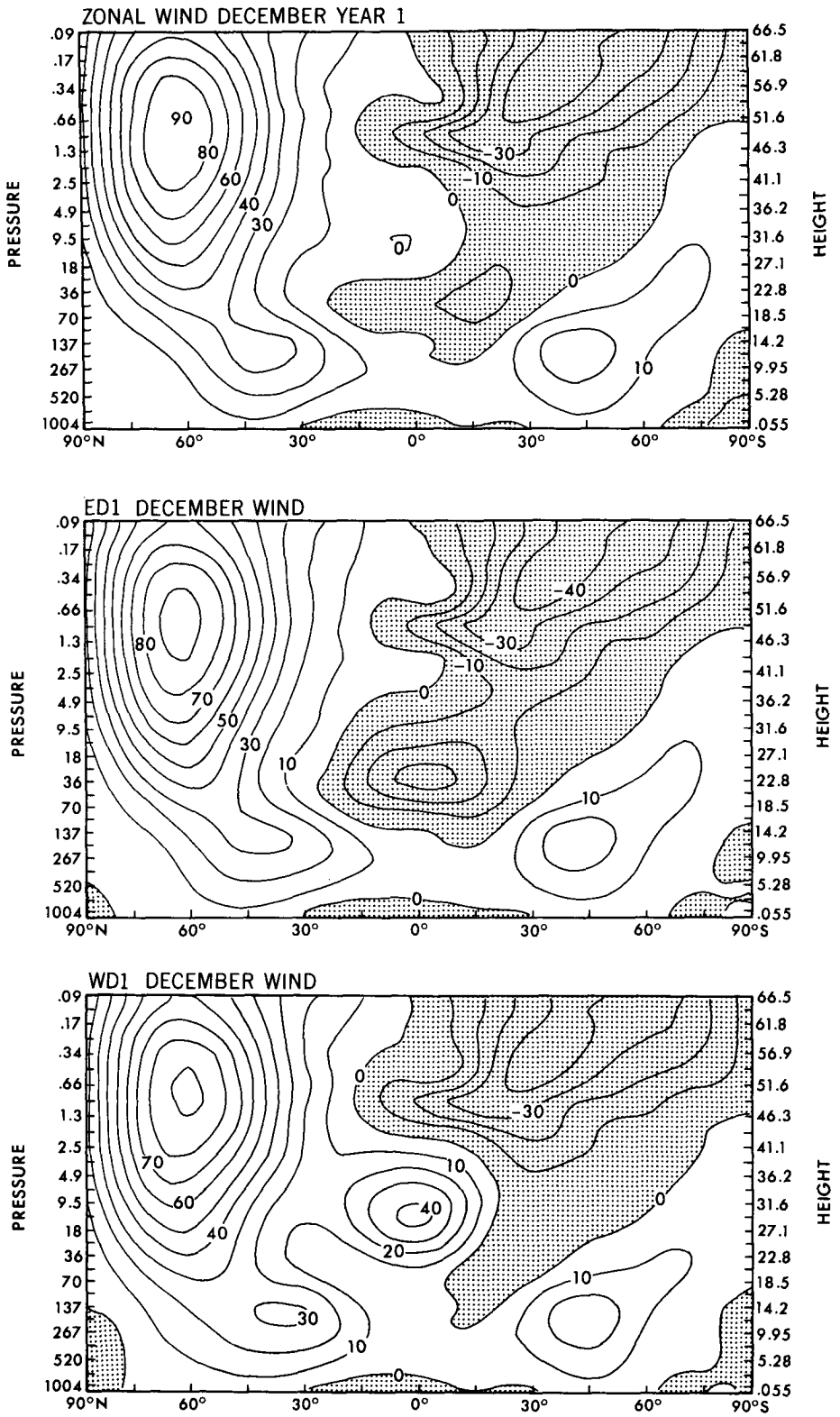


FIG. 14. Zonal-mean zonal winds averaged over December of year 1 for the control integration (top), the easterly perturbed experiment (middle), and the westerly perturbed experiment (bottom). The contour interval is 10 m $s^{-1}$ and easterlies are shaded.

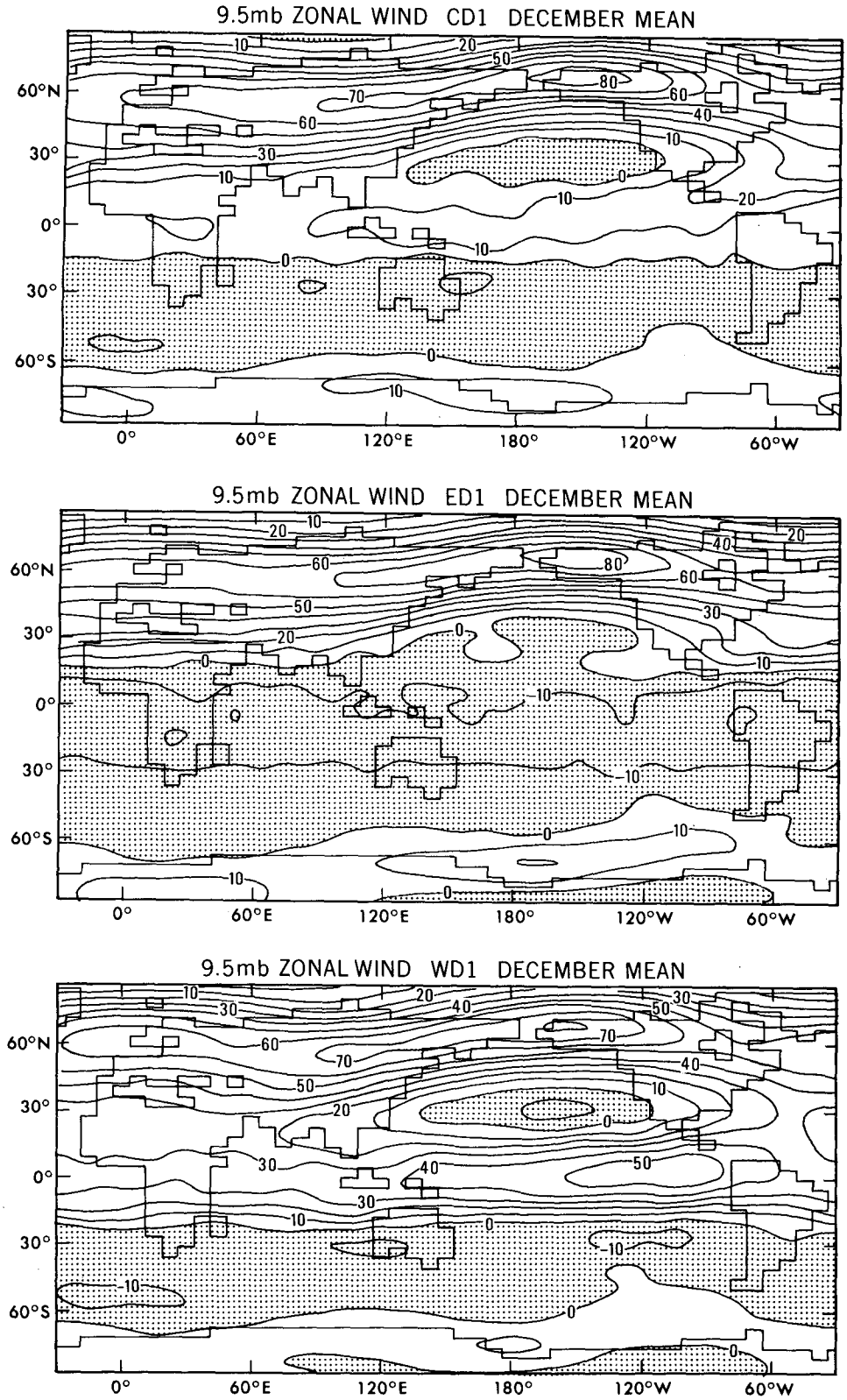


FIG. 15. Zonal winds at the 9.5-mb level averaged over December of year 1 for the control integration (top), the easterly perturbed experiment (middle), and the westerly perturbed experiment (bottom). The contour interval is 10 m $s^{-1}$ and easterlies are shaded.

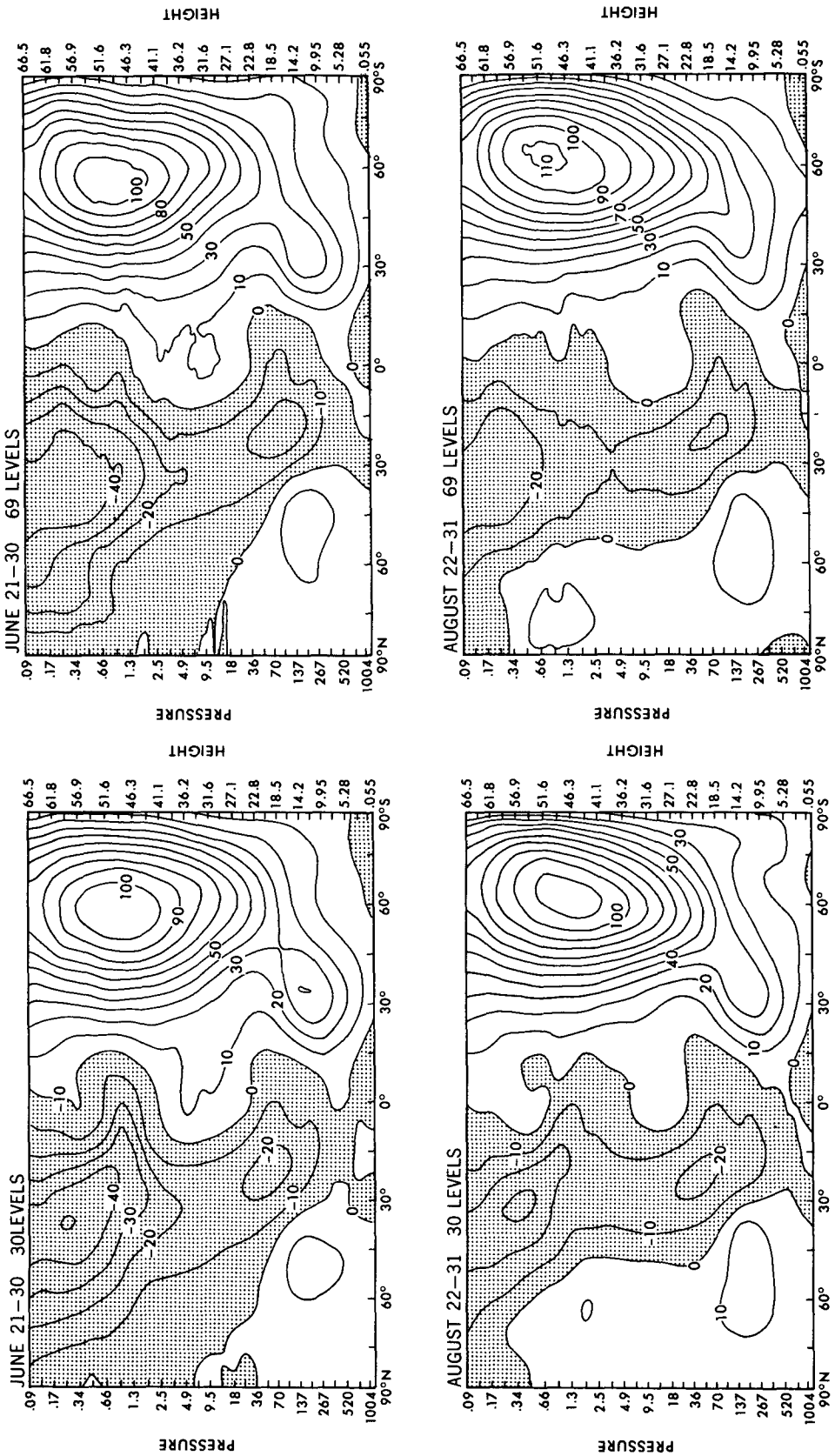


FIG. 16. Zonal-mean zonal wind averaged over ten-day periods for the 30-level model (left panels) and the 69-level model (right panels). The contour interval is 10 m $s^{-1}$ and easterlies are shaded.

changes in the general circulation might start to appear only at even finer vertical resolution. Nonetheless, the result shown in Fig. 16 is striking, and it suggests that the increased vertical resolution may not be the key to producing a QBO in a comprehensive GCM.

## 6. Conclusions

This paper has described a project in which a rhomboidal-15 spectral GCM was modified to investigate the processes maintaining the zonally averaged circulation in the equatorial stratosphere. The control integration of a 30-level version of the model was compared with experiments in which the tropical mean wind was strongly perturbed. There were some encouraging features in the results. The mean wind perturbations were found to relax with time scales of about one to a few months. The wind relaxations had downward propagation rather like QBO wind reversals, although this was much more pronounced above 30 km than at lower levels. The wind relaxation at levels above 30 km was largely caused by the "shadowing" effect of the mean flow on the vertically propagating waves (which actually produced mean wind anomalies of the opposite sign at sufficiently high levels). The GCM total vertical wave momentum fluxes in the lower stratosphere were found to be of comparable magnitude to those assumed in earlier mechanistic models of the QBO.

The model results suggest that the wave fluxes associated with quasi-stationary waves of midlatitude origin produce a significant easterly mean-flow driving in the equatorial stratosphere. The strong modulation of such fluxes by the zonal-mean zonal wind is a significant cause of the mean wind relaxation in the perturbation experiments. Below about 20 mb this effect is in fact the dominant driving of the mean-flow relaxations in both the May and December experiments.

A four-month segment of the GCM control integration was repeated with enhanced vertical resolution in the stratosphere. The evolution of the tropical mean winds was remarkably unaffected by this change in the model.

While some aspects of the model response to mean wind perturbations are encouraging, the fact remains that the GCM does not produce a QBO. The analysis of the model results points to two factors that could be involved in this deficiency. The fact that the upward wave fluxes into the equatorial stratosphere are spread over a wide range of both horizontal scales and zonal phase velocities may inhibit wave–mean flow interaction in the lower stratosphere. The strong influence of horizontal wave momentum transports from extratropical stationary waves may also militate against the production of a tropical mean-flow oscillation involving large $\bar{u}$ excursions from zero. The integration with the 69-level version of the model suggests that inadequate vertical resolution by itself may not explain the absence of a QBO in GCMs.

*Acknowledgments.* The authors would like to thank S. Manabe for encouraging them to use his model code for this study and for reviewing the manuscript. The assistance of R. T. Wetherald was invaluable in the process of adapting the model for these integrations. A. J. Broccoli, R. J. Stouffer, and W. Stern also provided important help. The authors are also grateful to J. D. Mahlman, Y. Hayashi, D. Rind, and an anonymous reviewer for their valuable comments on the manuscript.

## REFERENCES

Andrews, D. G., and M. E. McIntyre, 1976: Planetary waves in horizontal and vertical shear: the generalized Eliassen–Palm relation and the mean zonal acceleration. *J. Atmos. Sci.*, **33**, 2031–2048.

——, J. D. Mahlman, and R. W. Sinclair, 1983: Eliassen–Palm diagnostics of wave–mean flow interaction in the GFDL "SKYHI" general circulation model. *J. Atmos. Sci.*, **40**, 2768–2784.

Boville, B. A., 1985: The influence of damping on the winter lower stratosphere. *J. Atmos. Sci.*, **42**, 904–916.

——, and W. J. Randel, 1986: Observations and simulations of the stratosphere and troposphere in January. *J. Atmos. Sci.*, **43**, 3015–3034.

Crutcher, H. L., and J. M. Meserve, 1970: Selected level heights, temperatures and dew points for the Northern Hemisphere. NAVAIR 50-1C-52, U.S. Naval Weather Service, Washington, D.C.

Dickinson, R. E., 1969: Theory of planetary wave–zonal flow interaction. *J. Atmos. Sci.*, **26**, 73–81.

Dunkerton, T. J., 1983: Laterally propagating Rossby waves in the easterly acceleration phase of the quasi-biennial oscillation. *Atmos.–Ocean*, **21**, 55–68.

——, 1991: Nonlinear propagation of zonal winds in an atmosphere with Newtonian cooling and equatorial wave driving. *J. Atmos. Sci.*, **48**, 236–263.

——, and M. P. Baldwin, 1991: Quasi-biennial modulation of planetary wave fluxes in the Northern Hemisphere winter. *J. Atmos. Sci.*, **48**, 1043–1061.

——, C.-P. F. Hsu, and M. E. McIntyre, 1981: Some Eulerian and Lagrangian diagnostics for a model stratospheric sudden warming. *J. Atmos. Sci.*, **38**, 819–843.

Fels, S. B., J. D. Mahlman, M. D. Schwarzkopf, and R. W. Sinclair, 1980: Stratospheric sensitivity to perturbations in ozone and carbon dioxide: Radiative and dynamical response. *J. Atmos. Sci.*, **37**, 2265–2297.

Gordon, C. T., and W. F. Stern, 1982: A description of the GFDL global spectral model. *Mon. Wea. Rev.*, **110**, 625–644.

Hamilton, K., and J. D. Mahlman, 1988: General circulation model simulation of the semiannual oscillation of the tropical middle atmosphere. *J. Atmos. Sci.*, **45**, 3212–3235.

Hayashi, Y., 1971: A generalized method of resolving disturbances into progressive and retrogressive waves by space Fourier and time cross-spectral analysis. *J. Meteor. Soc. Japan*, **49**, 125–128.

——, 1974: Spectral analysis of tropical disturbances appearing in a GFDL general circulation model. *J. Atmos. Sci.*, **31**, 180–218.

——, D. G. Golder, and J. D. Mahlman, 1984: Stratospheric and mesospheric Kelvin waves simulated by the "SKYHI" general circulation model. *J. Atmos. Sci.*, **41**, 1971–1984.

Hirota, I., 1978: Equatorial waves in the upper stratosphere mesosphere in relation to the semiannual oscillation of the zonal wind. *J. Atmos. Sci.*, **35**, 714–722.

Holton, J. R., and R. S. Lindzen, 1972: An updated theory for the

quasi-biennial cycle of the tropical stratosphere. *J. Atmos. Sci.*, **29,** 1076–1080.

——, and H. C. Tan, 1980: The influence of the equatorial quasi-biennial oscillation on the global circulation at 50 mb. *J. Atmos. Sci.*, **37,** 2200–2208.

——, and ——, 1982: The quasi-biennial oscillation in the Northern Hemisphere lower stratosphere. *J. Meteor. Soc. Japan,* **60,** 140–148.

Kasahara, A., and T. Sasamori, 1974: Simulation experiments with a 12-layer atmospheric general circulation model. II Momentum balance and energetics in the stratosphere. *J. Atmos. Sci.*, **31,** 408–421.

Lindzen, R. S., 1971: Equatorial planetary waves in shear: Part I. *J. Atmos. Sci.*, **29,** 1452–1463.

——, and J. R. Holton, 1968: A theory of the quasi-biennial oscillation. *J. Atmos. Sci.*, **25,** 1095–1107.

——, and C.-Y. Tsay, 1975: Wave structure of the tropical stratosphere over the Marshall Islands area during 1 April–1 July 1958. *J. Atmos. Sci.*, **32,** 2009–2021.

Ma, C.-C., 1990: Models of planetary wave propagation in the middle atmosphere. Pd.D. dissertation, Princeton University, Princeton, New Jersey, 118 pp.

Manabe, S., and B. G. Hunt, 1968: Experiments with a stratospheric general circulation model: I radiative and dynamic aspects. *Mon. Wea. Rev.*, **96,** 477–502.

——, and J. D. Mahlman, 1976: Simulation of seasonal and interhemispheric variations in the stratospheric circulation. *J. Atmos. Sci.*, **33,** 2185–2217.

——, D. G. Hahn, and J. L. Holloway, Jr., 1979: Climate simulations with GFDL spectral models of the atmosphere: effect of spectral truncation. Report of the JOC study conference on climate models: Performance, intercomparison and sensitivity studies. Vol. 1. W. L. Gates, Ed., *GARP Publ. Ser.* **22,** 41–94.

Plumb, R. A., 1977: The interaction of two internal gravity waves with the mean flow: Implications for the theory of the quasi-biennial oscillation. *J. Atmos. Sci.*, **34,** 1847–1858.

——, and R. C. Bell, 1982: A model of the quasi-biennial oscillation on an equatorial beta-plane. *Quart. J. Roy. Meteor. Soc.*, **108,** 335–352.

Salby, M. L., D. L. Hartmann, P. L. Bailey, and J. C. Gille, 1984: Evidence for equatorial Kelvin modes in *Nimbus-7* LIMS. *J. Atmos. Sci.*, **41,** 220–235.

Saravanan, R., 1990: A multiwave model of the quasi-biennial oscillation. *J. Atmos. Sci.*, **47,** 2465–2474.

Taljaard, J. J., H. van Loon, H. L. Crutcher, and R. L. Jenne, 1969: Climate of the upper air, 1. Southern Hemisphere. Vol. 1. NAVAIR 50-1C-55, U.S. Naval Weather Service, Washington, D.C.

Yanai, M., and T. Maruyama, 1966: Stratospheric wave disturbances propagating over the equatorial Pacific. *J. Meteor. Soc. Japan,* **44,** 291–294.